COMBUSTION AND FLAME 60: 15-28 (1985)

A Lagrangian Sectional Approach for Simulating Droplet Size Distribution of Vaporizing Fuel Sprays in a Turbulent Jet*

YORAM TAMBOUR

Department of Aeronautical Engineering, Technion-Israel Institute of Technology, Haifa 32000, Israel.

A new Lagrangian sectional approach is used to analyze spray vaporization in a turbulent air jet flow. The fuel is considered to be in the form of discrete liquid droplets which have an arbitrary range of sizes and differ in their rates of vaporization. Assuming that the droplets follow the flow streamlines, the "residence time" of droplets as a function of the spatial coordinates is computed via the fluid Eulerian velocity field. Then, following a "group" of vaporizing droplets along a streamline, the Lagrangian approach is used. To avoid the dimensionality problem associated with the discrete form of the droplet population balance equations, "sectional conservation equations" are employed. Simulation of the downstream changes in volume distribution of fuel droplets of a vaporizing spray produced by an air-kerosene jet atomizer is presented. The theoretically predicted results of this simulation show good agreement with experimentally reported data.

INTRODUCTION

Both experimental [1, 2] and analytical [3, 4] results show that in most practical situations, spray burning, rather than being controlled by "single droplet burning," is a "droplet cloud" process, in which the majority of droplets vaporize in groups and reaction occurs at the vapor/air interface surrounding the clouds, similar to a gas diffusion flame. Thus, modeling of spray burning requires modeling of cloud droplet vaporization and droplet-flow interaction under conditions of heat and mass transfer between the droplets and the surrounding gas which do not generally involve regions of reaction close to the droplet surface. Furthermore the "cloud vaporization" process which generally occurs for most liquid fuel sprays ensures that the environment (and thus the vaporization and ballistics) of each individual droplet is controlled by the vaporization and ballistics of many surrounding droplets.

The performance of a combustion unit is critically dependent upon the drop size produced by the atomizer and the manner in which the combustion air mixes with the droplets. In the jet engine afterburning process, a critical factor for combustion efficiency and stability is the "residence time" of droplets in the afterburner, i.e., the average time droplets take to travel from the injectors downstream (toward the flameholders) up to the point of complete vaporization. In a similar manner, "residence time" of droplets is also important in the analysis of the performance of the main combustion chamber of jet engines, in liquid-fuel rocket motors, diesel engines, and industrial pressure jet burners.

Early theoretical analyses of spray combustion were presented by Probert [5] and by Tanasawa and Tesima [6]. Probert calculated the influence of spray droplet size on the rate of combustion. He used the Rosin-Rammler distri-

* This research was supported by Technion V. P. R. Fund-Seniel Ostrow Research Fund.

Published by Elsevier Science Publishing Co., Inc.
52 Vanderbilt Avenue, New York, NY 10017

0010-2180/85/$03.30

bution law, which was also used later by Nuruzzaman et al. [7]. Another analysis, by Mizutani and Ogasawara [8], is based on a one-dimensional flame model which assumes that all the droplets in one plane ignite at the same instant and the flames surrounding each droplet are replaced by a hypothetical planar flame front.

Recently, Correa and Sichel [9] analyzed a monodisperse spherical fuel cloud in equilibrium with a quiescent atmosphere. A polydisperse size distribution of droplets has been considered by Choudhury and Gerstein [10], who analyzed time variations in size distribution of droplets. However, the vaporization of fuel droplets was considered only in a stagnant atmosphere without flow, and the initial size distribution, although being polydisperse, was not arbitrary but given by a certain analytical function. Yet some of the results of Choudhury and Gerstein are in agreement with earlier work by Tambour [11] in which an arbitrary size distribution was employed.

For a detailed understanding of the process of spray combustion, it is necessary first to have knowledge of (i) the mechanism of vaporization of the individual droplets and (ii) the size and spatial distribution of the droplets that make up the spray. Of these, the mechanism of single droplet vaporization and combustion is fairly well established in the literature [12–17], theoretically and experimentally. The *initial* size and spatial distribution can be determined by experimental methods such as shadowgraph photographs, laser holography, laser tomography, and pulse counting techniques [18–23]. Thus, theoretical simulation of a whole spray of a wide range of sizes is possible in principle. The complexity of the problem lies in the fact that the flow field is mostly turbulent and the total number of discrete droplet sizes needed to simulate actual fuel sprays can be immense.

To avoid the dimensionality problem associated with the discrete form of population balance equations of the fuel spray droplets, "sectional conservation equations" have been previously presented by the author [11], [24]. The method, based on dividing the droplet size domain into sections and dealing only with one integral quantity in each section (e.g., number, surface area of droplets, or volume), has the advantage that the integral quantity is conserved within the computational domain and the number of conservation equations is substantially reduced to be simply equal to the number of sections. Using an *Eulerian approach,* this sectional method has been employed previously to analyze the droplet size distribution in a laminar boundary-layer flow field [24]. The Eulerian approach has some computational advantages, as demonstrated in the above reference. However, for comparison of theoretical predictions with experimental data, a *Lagrangian approach* is physically more meaningful when dealing with droplet populations. It also allows one to analyze the relative contributions of various factors to the changes in the droplet size distribution following the "same" group of droplets. Thus, in the present study a new sectional Lagrangian approach for simulating a turbulent air-jet fuel atomizer is presented.

FLOW FIELD GOVERNING EQUATIONS

The purpose of the present study is to simulate the downstream changes in volume distribution of fuel droplets suspended in a turbulent air-jet flow. Thus, in this section we begin with the analysis of the air-jet flow field. The governing equations for an axisymmetric steady-state turbulent gas jet flow can be written as

continuity:

$$\frac{\partial}{\partial x}(\rho u)+\frac{1}{r}\frac{\partial}{\partial r}(r\rho v)=0; \tag{1}$$

momentum:

$$\rho u\frac{\partial u}{\partial x}+\rho v\frac{\partial u}{\partial r}=\frac{1}{r}\frac{\partial}{\partial r}\left(r\mu_{\text{eff}}\frac{\partial u}{\partial r}\right); \tag{2}$$

energy:

$$\rho u\frac{\partial h_t}{\partial x}+\rho v\frac{\partial h_t}{\partial r}=-\frac{1}{r}\frac{\partial}{\partial r}(rJ_{qr}) +\frac{1}{r}\frac{\partial}{\partial r}\left[r\mu_{\text{eff}}\left(1-\frac{1}{\text{Pr}_{\text{eff}}}\right)\times\frac{\partial}{\partial r}\left(\frac{u^2}{2}\right)\right]-\dot{S}_L; \tag{3}$$

here ρ is the density, u and v are the axial and radial velocity components, respectively, x is the distance along the jet axis, r is the radial coordinate (see Fig. 1), μ_{eff} is the effective shear viscosity, h_t is the specific total enthalpy, J_{qr} is the energy flux in the radial direction, Pr_{eff} is the effective Prandtl number, and $\dot{S}_{\text{L}}$ is the energy used for latent heat of vaporization of droplets suspended in the gas flow. The use of the effective transport properties μ_{eff} and Pr_{eff} is discussed in Ref. [25].

The boundary conditions for the velocity and temperature fields are as follows:

$$\begin{aligned}
&\text{at } r=0: \quad v=0, \quad \frac{\partial u}{\partial r}=0, \quad \frac{\partial T}{\partial r}=0;\\
&\text{at } r\to\infty: \quad v=0, \quad u=u_\infty, \quad T=T_\infty;\\
&\text{for } x=x_0, \text{ at } r=0: \quad u=u_0, \quad T=T_0; \qquad (4)
\end{aligned}$$

here x_0 is a certain downstream distance from the outlet of the atomizer for which full disintegration has already occurred.

Solution procedures for the velocity and temperature fields can be found in the literature [25–27]. As to the droplet size distribution field, a Lagrangian representation will be presented in the next section. Assuming that the droplets follow the flow streamlines, calculations will be carried out to obtain streamlines and residence time of droplets. These calculations will be based on the solutions for the velocity field and will involve numerical integration of the velocity components u and v for short time increments Δt (see Fig. 1).

LAGRANGIAN REPRESENTATION FOR THE SPRAY

For the droplet population, we employ here a Lagrangian representation as follows. We denote a control volume which contains a group of droplets which are given a fixed identity by specifying their initial position (x_0, r_{I}) at a given time $t_0 = 0$; then, we follow "the same" group of droplets along a streamline, assuming that droplets follow the fluid velocity field. The validity of this assumption will be discussed later when we compare our theoretical results with experimental data.

To enable simulation of the complex droplet size distributions observed in practical cases, the spray is considered to be comprised of droplets of an arbitrary range of sizes which differ in their rate of vaporization. In the Lagrangian representation, the size distribution of the spray droplets can be described by the concentration of discrete droplets of various sizes per unit volume of fluid $n_i(t)$. This concen-

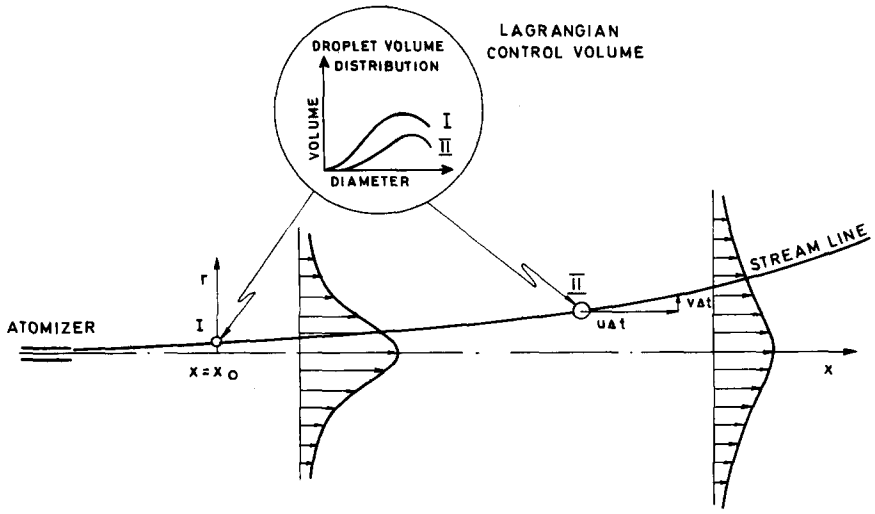

Fig. 1. Geometry and coordinates.

tration varies along a streamline (due to the vaporization process) as a function of the droplets residence time t and the changes in the temperature field along their path. The subscript i denotes an integer ($i = 1, 2, \cdots$); i.e., it is assumed that each droplet consists of an integer multiple of monomers, where a monomer can be described as a single molecule of the species comprising the droplet [11].

The vaporization process can be described by a set of coupled differential equations for $n_1(t)$, $n_2(t)$, etc. The concentration conservation equation for each i-mer (i.e., droplets which consist of i monomers) is given by

$$\frac{dn_i}{dt} = -E_i n_i + E_{i+1} n_{i+1}, \qquad i = 1, 2, 3, \cdots, \tag{5}$$

where E_i is the frequency of molecule evaporation from an i-mer droplet. Functional forms of this frequency can be obtained through known expressions of vaporization rates of single droplets or may be determined through correlations with known experimental results of measured vaporization rates [13, 28]. From theoretical and experimental data, it is obvious that E_i highly depends on the diameter of the i-mer droplet and on the temperature of the surrounding gas in addition to other parameters. Thus, in the above Lagrangian representation, Eq. (5), E_i changes for each time increment Δt, according to the Eulerian flow and temperature fields.

In general, the total number of discrete droplet sizes, i.e., the magnitude of the integer i, needed to simulate actual fuel sprays can be immense. To avoid the dimensionality problem associated with the discrete form of population balance equations, we follow the method of Ref. [24] and use here sectional conservation equations which are presented below. The method is based on dividing the droplet size domain into sections and dealing only with one integral quantity in each section (e.g., number, surface area of droplets, or volume). This sectional representation has the advantage that the integral quantity is conserved within the computational domain and the number of conservation equations is substantially reduced to be simply equal to the number of sections.

SECTIONAL INTEGRAL SPRAY PROPERTY $Q_j(t)$

In the analysis of spray vaporization, not only the number concentration of droplets is important but their surface area and their volume are important as well. Thus, we introduce a general property of the spray,

$$q_i(t) = i^\gamma n_i(t), \tag{6}$$

where γ is equal to zero, or unity, or $\gamma = 2/3$, depending on the property of interest. For example: for $\gamma = 0$, q_i is simply equal to the number concentration $n_i(t)$; for $\gamma = 1$, q_i is proportional to the volume or mass within the i-mer droplets; and for $\gamma = 2/3$, q_i is proportional to the surface area of the droplets.

Then following Ref. [24], we divide the entire droplet size domain into m arbitrary sections, and define $Q_j(t)$ to be an integral quantity of the spray within the jth section. This is

$$Q_j(t) = \sum_{i=k_{j-1}+1}^{k_j} i^\gamma n_i(t), \qquad j = 1, 2, 3, \cdots, m, \tag{7}$$

where $k_{j-1}+1$ and k_j denote the number of monomers in the smallest and largest droplets, respectively, in the jth section (where $k_0 = 0$).

Due to the vaporization process, the size of the droplets is reduced. Thus, the change in q due to the evaporation of a molecule from an i-mer droplet is $i^\gamma - (i-1)^\gamma$. Whenever i-mer droplets leave section j due to a vaporization process, Q_j is reduced by $E_i n_i i^\gamma$. However, Q is also increased in lower sections due to the vaporization of droplets in higher sections. Droplets which contained $(k_j + 1)$ monomers before the vaporization process will "join" the jth section after evaporation of a molecule, increasing Q_j by $E_{k_j+1} n_{k_j+1} (k_j)^\gamma$. Thus the decrease of the integral quantity Q within section j due to the vaporization process may be ex-

pressed as

$$\frac{dQ_j}{dt} = -\sum_{i=k_{j-1}+1}^{k_j} E_i[i^\gamma - (i-1)^\gamma] n_i(t) - E_{k_{j-1}+1}(k_{j-1})^\gamma n_{k_{j-1}+1}(t) + E_{k_j+1}(k_j)^\gamma n_{k_j+1}(t). \quad (8)$$

The first term on the right-hand side of Eq. (8) expresses the decrease in Q_j due to the size reduction of all droplets within section j. Now, droplets (within section j) which contain $(k_{j-1}+1)$ monomers will leave section j after a molecule evaporates. This is described by the second term in the equation. The third term is due to the droplets added to section j from section $(j+1)$.

To express dQ/dt) in terms of Q_j, $j = 1, 2, \cdots, m$, it is necessary to use the fundamental approximation inherent in sectional representations; i.e., one may choose some functional forms of the distribution within the sections such that the integral quantity of interest remains equal to Q_j for all sections $j = 1, 2, \cdots, m$. Thus, according to Eq. (7)

$$n_{k_{j-1}+1}(t) = \frac{Q_j(t)}{(k_{j-1}+1)^\gamma (k_j - k_{j-1})} \quad (9)$$

and

$$n_{k_j+1}(t) = \frac{Q_{j+1}(t)}{(k_j+1)^\gamma (k_{j+1} - k_j)} . \quad (10)$$

Now, employing Eqs. (9), (10), and (7), Eq. (8) finally becomes

$$\frac{dQ_j}{dt} = -C_j Q_j + B_{j,j+1} Q_{j+1} \qquad j = 1, 2, \cdots, m, \quad (11)$$

where the sectional coefficients $B_{j,j+1}$ and C_j are described as follows:

$$B_{j,j+1} = \left(\frac{k_j}{k_j+1}\right)^\gamma \frac{E_{k_j+1}}{k_{j+1} - k_j} , \quad (12)$$

$$C_j = \left(\frac{k_{j-1}}{k_{j+1}+1}\right)^\gamma \frac{E_{k_{j-1}}+1}{k_j - k_{j-1}} + \frac{1}{k_j - k_{j-1}} \times \sum_{i=k_{j-1}+1}^{k_j} \frac{1}{i^\gamma} E_i[i^\gamma - (i-1)^\gamma]. \quad (13)$$

The functional form used to describe the rate of vaporization E_i, in order to evaluate these sectional coefficients, will be discussed later. In the next section, a general solution procedure for the set of the sectional Lagrangian Eqs. (11) is presented.

SOLUTION OF THE LAGRANGIAN EQUATIONS

Solutions for the Lagrangian sectional conservation equations will be derived for an arbitrary number of sections and sectional divisions, subject to any arbitrary initial distribution of $Q_j(0)$, $j = 1, 2, \cdots, m$.

The set of coupled differential equations described by Eq. (11) may be rewritten in a matrix form as

$$\frac{d}{dt}\begin{bmatrix} Q_1 \\ Q_2 \\ Q_3 \\ \cdot \\ \cdot \\ \cdot \\ Q_{m-1} \\ Q_m \end{bmatrix} = \begin{bmatrix} -C_1 & B_{1,2} & 0 & 0 & \cdots & 0 & 0 \\ & -C_2 & B_{2,3} & 0 & \cdots & 0 & 0 \\ & & -C_3 & B_{3,4} & \cdots & 0 & 0 \\ & & & & & \cdot & \cdot \\ & & & & & \cdot & \cdot \\ & & & & & \cdot & \cdot \\ 0 & & & & & -C_{m-1} & B_{m-1,m} \\ & & & & & & -C_m \end{bmatrix} \begin{bmatrix} Q_1 \\ Q_2 \\ Q_3 \\ \cdot \\ \cdot \\ \cdot \\ Q_{m-1} \\ Q_m \end{bmatrix} \quad (14)$$

These are the sectional conservation equations for the integral quantity Q_j for which we assume here a general solution of the form

$$\begin{bmatrix} Q_m(t) \\ Q_{m-1}(t) \\ \cdot \\ \cdot \\ \cdot \\ Q_2(t) \\ Q_1(t) \end{bmatrix} = \begin{bmatrix} & & & & 0 \\ & & & & \\ & & & & \\ & & & & \\ & & \omega_{2,2} & \omega_{3,2} & \cdots \\ \omega_{1,1} & \omega_{2,1} & \omega_{3,1} & & \cdots \end{bmatrix} \begin{bmatrix} & & & \omega_{m,m} \\ & & & \omega_{m,m-1} \\ \omega_{m-1,m-1} & & & \cdot \\ \cdot & & & \cdot \\ \cdot & & & \cdot \\ \cdot & & & \omega_{m,2} \\ & & & \omega_{m,1} \end{bmatrix} \begin{bmatrix} e^{-C_1 t} \\ e^{-C_2 t} \\ \cdot \\ \cdot \\ \cdot \\ e^{-C_{m-1} t} \\ e^{-C_m t} \end{bmatrix}, \quad (16)$$

where the coefficients ω_{ij} are to be found.

First, we begin with the solution for the highest section $j = m$, since the solution for any lower section is coupled to solutions of all the higher sections. The solution for $Q_m(t)$ is

$$Q_m(t) = \omega_{m,m} \exp(-C_m t), \quad (17)$$

where

$$\omega_{m,m} = Q_m(0). \quad (18)$$

Then, by substituting the general solution Eq. (16) into Eq. (14), and by equating the terms with like powers of the exponent, the coefficients ω_{ij} for the sections lower than m are obtained. Thus, beginning with section $j = m - 1$, employing in each section the known solutions of the higher sections and satisfying the initial conditions for $Q_j(0)$, we derive the following general recursion formulas:

for $i > j$:

$$\omega_{i,j} = -\frac{B_{j,j+1}}{C_i - C_j} \omega_{i,j+1}; \quad (19)$$

for $i = j$:

$$\omega_{jj} = Q_j(0) - \sum_{\nu=j+1}^{m} \omega_{\nu,j}. \quad (20)$$

Thus, for example, to determine the coefficients for the solution of $Q_{m-1}(t)$, we employ the known value of $\omega_{m,m}$, Eq. (18), and evaluate

$$Q_j(t) = \sum_{i=j}^{m} \omega_{ij} \exp(-C_i t), \quad (15)$$

which in a matrix notation may be rewritten as

$\omega_{m,m-1}$ via Eq. (19):

$$\omega_{m,m-1} = -\frac{B_{m-1,m}}{C_m - C_{m-1}} \omega_{m,m}. \quad (21)$$

Then, $\omega_{m-1,m-1}$ is determined through Eq. (20),

$$\omega_{m-1,m-1} = Q_{m-1}(0) - \omega_{m,m-1}, \quad (22)$$

by which the initial condition $Q_{m-1}(0)$ is satisfied, etc.

Computed results for the downstream changes in volume distribution of fuel droplets of a vaporizing spray in a turbulent jet flow will be presented below. Once the solutions for the Eulerian flow field are obtained, a numerical integration along streamlines is carried out. This integration is based on downstream marching in short time increments $\Delta t (= 5 \times 10^{-5}$ s), beginning at the initial cross section x_0 (see Fig. 1). After each step, the new spatial location is determined by integration of the velocity components u and v, while the new droplet size distribution is determined via Eq. (16). As to the functional form that is used in the present study for the evaluation of the sectional vaporization coefficients, this subject is discussed next.

EVALUATION OF THE SECTIONAL VAPORIZATION COEFFICIENTS

As is evident from Eqs. (12) and (13) the magnitudes of the sectional coefficients $B_{j,j+1}$ and C_j depend on the limits of each section j and

on the functional form used to describe the vaporization rate of a single droplet of volume v. To evaluate these coefficients, we find it more convenient to first express the summation in Eq. (13) by an integral. To do so, we express Q_j [see Eq. (7)] as

$$Q_j = \int_{v_{j-1}}^{v_j} v^\gamma n(v, t)\, dv, \tag{23}$$

where $n(v, t)$ is the number concentration function and v_{j-1} and v_j denote the volumes of the smallest and largest droplets, respectively, in section j.

By means of these definitions, the coefficients $B_{j,j+1}$ and C_j can be written, respectively, as

$$B_{j,j+1} = \left(\frac{v_{k_j}}{v_{k_j+1}}\right)^\gamma \frac{E(v_j, T)}{v_{j+1} - v_j}, \tag{24}$$

$$C_j = \left(\frac{v_{k_{j-1}}}{v_{k_{j-1}+1}}\right)^\gamma \frac{E(v_{j-1}, T)}{v_j - v_{j-1}} + \frac{1}{v_j - v_{j-1}} \int_{v_{j-1}}^{v_j} \frac{1}{v^\gamma} E(v, T)\, dv^\gamma, \tag{25}$$

where $E(v, T)$ is the volume rate of vaporization of a droplet of volume v.

Next, we take the mass or volume rate of vaporization of each single droplet to be proportional to the droplet diameter d (the d^2 law). Thus,

$$E(v, T) = (\pi/4)E(T)d, \tag{26}$$

where $E(T)$ is the vaporization or burning rate coefficient, which depends on the temperature differential between the droplet and the surrounding gas, the diffusivity and other properties of the fuel, and its surroundings. That is, the dependence of the vaporization rate $E(v, T)$ on the fuel type and the surrounding conditions is completely contained in $E(T)$. Several models for evaluating $E(T)$, for various operating conditions, have been summarized in a comprehensive review by Williams [13]. For instance, for a stationary single droplet of a uniform and constant temperature, $E(T)$ reduces to the known burning rate constant (usually denoted in the literature by K [13]). However, even under transient temperature conditions, the d^2 law has been found [29, 30, 31] to yield reasonably accurate estimates for droplet size and vaporization time.

For interacting fuel droplets, a correction factor (η) may be used in the d^2 law as suggested by Labowsky [31]. Generally, the vaporization rate of a droplet decreases when this droplet is part of a group of vaporizing droplets. Thus, the d^2 law tends to overestimate the droplet life time. However, the d^2 law does predict the actual vaporization history of the interacting droplet, especially in the initial period of combustion [31]. In order to determine $E(T)$ for a group of vaporizing droplets, one may also resort to experimental data, e.g., data which show downstream changes in jet spray characteristics. A detailed procedure to demonstrate this is presented in the Appendix.

Next, we employ the d^2 law as expressed by Eq. (26) to reexpress the sectional vaporization coefficients. Thus, substituting Eq. (26) into Eqs. (23) and (24), and denoting by d_{Lj} and d_{Uj} the lower and upper diameter limits of section j, one obtains the following sectional coefficients for an integral property Q_j which represents the *integral surface area* of droplets in section j:

$$B_{j,j+1}{}^s = \frac{3}{2} E(T) \left(\frac{d_{Uj}}{d_{L,j+1}}\right)^2 \frac{d_{L,j+1}}{d_{U,j+1} - d_{U,j}{}^3}, \tag{27}$$

$$C_j{}^s = \frac{3}{2} E(T) \left[\left(\frac{d_{U,j-1}}{d_{Lj}}\right)^2 \frac{d_{Lj}}{d_{U,j+1}{}^3 - d_{U,j-1}{}^3} + \frac{2(d_{Uj} - d_{Lj})}{d_{Uj}{}^3 - d_{U,j-1}{}^3}\right]. \tag{28}$$

Notice that the superscript s denotes surface area. For Q_j, which represents the *integral volume* of droplets in section j, the sectional vaporization coefficients become

$$B_{j,j+1}{}^v = \frac{3}{2} E(T) \left(\frac{d_{Uj}}{d_{L,j+1}}\right)^3 \frac{d_{L,j+1}}{d_{U,j+1}{}^3 - d_{U,j}{}^3}, \tag{29}$$

$$C_j^v=\frac{3}{2}E(T)\left[\left(\frac{d_{U,j-1}}{d_{Lj}}\right)^3\frac{d_{Lj}}{d_{Uj}^3-d_{U,j-1}^3}+\frac{3(d_{Uj}-d_{Lj})}{d_{Uj}^3-d_{U,j-1}^3}\right]. \quad (30)$$

For a continuous division into sections whereby $d_{U,j-1} \rightarrow d_{L,j}$ and $d_{Uj} \rightarrow d_{L,j+1}$, both sets of coefficients may be rewritten as

$$B_{j,j+1}=\frac{3}{2}E(T)\frac{d_{L,j+1}}{d_{U,j+1}^3-d_{L,j+1}^3}, \quad (31)$$

$$C_j=\frac{3}{2}E(T)\left[\frac{d_{Lj}}{d_{Uj}^3-d_{Lj}^3}+\frac{3\gamma(d_{Uj}-d_{Lj})}{d_{Uj}^3-d_{Lj}^3}\right], \quad (32)$$

where $\gamma = 2/3$ for surface area distributions, whereas $\gamma = 1$ for droplet volume distributions. For droplet number distributions, the second term in Eq. (32) vanishes since $\gamma = 0$ [see also Eq. (13)].

In the present study, the droplet size domain is divided into two overlapping divisions, with each division including 5 sections as follows. The first division: 0–30, 30–60, 60–90, 90–120, 120–150 μm; and the second division: 1.5–6.5, 6.5–11.5, 11.5–16.5, 16.5–21.5, 21.5–26.5 μm. For $E(T)$, the value of 9.8×10^3 $\mu m^2/s$ was used. This value was obtained directly from experimental data by a calculation based on two peak values of downstream changes of droplet volume concentrations, as explained in the Appendix. The sectional coefficients were evaluated via Eqs. (31) and (32) and are presented in Table 1.

RESULTS OF SIMULATION AND DISCUSSION

In this section, we employ our theory to simulate experimental results of downstream changes in volume distribution of fuel droplets produced by an air–kerosene jet atomizer. Comprehensive experimental data on this topic have been reported by a group of researchers: Yule et al. [19] and recently Yule et al. [23]. In the experiments described in Ref. [19], a twin fluid atomizer was used to produce a kerosene spray injected into a coflowing secondary stream. Measurements were made for two flow conditions: (i) "cold" secondary air (293K) and cold atomizing air with kerosene, (ii) hot secondary air (450K) and cold atomizing air with kerosene. The sprays for both the cold and hot cases had the same initial conditions as specified below: mass flow rate of kerosene = 0.072 g/s, nozzle

TABLE 1

Sectional Vaporization Coefficients for Droplet Volume and Droplet Surface Area Distributions Normalized by the Volume Rate Vaporization Coefficient $E(T)$

Droplet Diameter (μm)	$C_j^v/E(T)$ (μm^{-2})	$C_j^s/E(T)$ (μm^{-2})	$B_{j,j+1}^{v,s}/E(T)$ (μm^{-2})
1.5- 6.5	0.0912442	0.0635945	0.0078235
6.5–11.5	0.0258776	0.0198596	0.0058056
11.5–16.5	0.0133782	0.0108540	0.0045444
16.5–21.5	0.0086757	0.0072986	0.0037192
21.5–26.5	0.0063140	0.0054490	—
0- 30	4.99999×10^{-3}	3.333333×10^{-3}	0.238093×10^{-3}
30- 60	0.95238×10^{-3}	0.714285×10^{-3}	0.175438×10^{-3}
60- 90	0.43859×10^{-3}	0.350877×10^{-3}	0.135135×10^{-3}
90–120	0.27027×10^{-3}	0.225225×10^{-3}	0.109288×10^{-3}
120–150	0.19125×10^{-3}	0.163932×10^{-3}	—

outlet i.d. = 0.5 mm, mass flow rate of atomizing air 0.187 g/s flowing through an annular cross section at the nozzle outlet, i.d. = 0.65 mm and o.d. = 1.5 mm, average velocity of atomizing air at atomizer nozzle = 105 m/s, cold secondary air velocity = 5 m/s and hot second air velocity = 7.3 m/s.

The computed axial velocity profiles at a cross-sectional plane which is located at a distance of x = 100 mm downstream (measured from the nozzle outlet) are presented in Fig. 2 for both the "cold" and "hot" flows. A kinematic effective viscosity of $\nu_{\text{eff}} = 6.38 \times 10^{-3}$ m^2/s was used in the calculations, and the axial momentum was taken to be $K_c' = 6.414 \times 10^{-2}$ m^4/s^2 and $K_h' = 7.865 \times 10^{-2}$ m^4/s^2, for the "cold" and "hot" flows, respectively. The computed results show good agreement when compared with experimental measurements of the axial gas velocity and the average axial velocity of the droplets at the above location. This agreement is due to the fact that in the above experiment, fine sprays were reported to be utilized. Thus, as these experimental results indicate, the phenomenon of droplet/gas velocity lag occurs mainly near the nozzle outlet. In the vicinity of the nozzle outlet, the droplets accelerate due to the atomizing air stream. This acceleration occurs up to some distance downstream, from where on most of the droplets follow the local gas velocity field. Thus, from a certain distance downstream, the assumption that droplets follow the streamlines is valid for fine sprays.

As to the simulation of downstream changes in volume distribution of droplets, results (normalized by an arbitrary reference volume) are presented in Figs. 3 and 4 for the "cold" and "hot" flows, respectively. In order to carry out computations for these simulations it is imperative to start the calculations from a given initial volume distribution of droplets at a certain cross-sectional plane upstream. This initial distribution must be determined from experimental data. Once this initial distribution is known, theoretical predictions of the downstream changes of the droplet volume distribution can be made, as indicated in the present study. As shown in Figs. 3 and 4, the theoretical predictions for the downstream changes of droplet volume distribution show satisfactory agreement with the reported experimental data. The "width" of the droplet distribution profiles increases somewhat as one marches downstream. This is attributed to the fact that the streamlines (carrying the droplets) are shifting from the center of the jet.

In the "hot" flow case, droplet vaporization rate is higher than that for the "cold" flow. Thus, in Fig. 4, for the "hot" flow, we also presented computed results which took into account the decrease in the local gas temperature

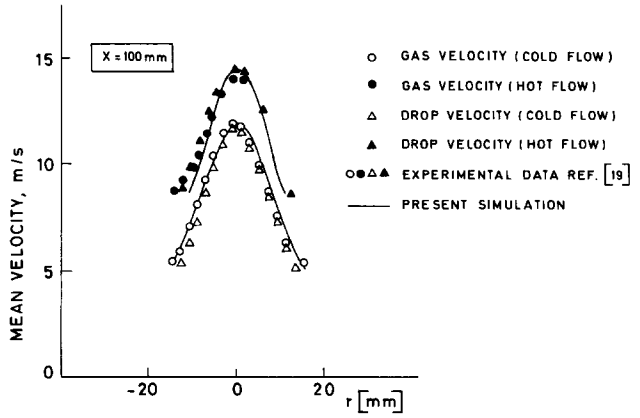

Fig. 2. Axial velocity distributions for gas and droplets at a cross-sectional plane at x = 100 mm for both the "cold" and "hot" flows.

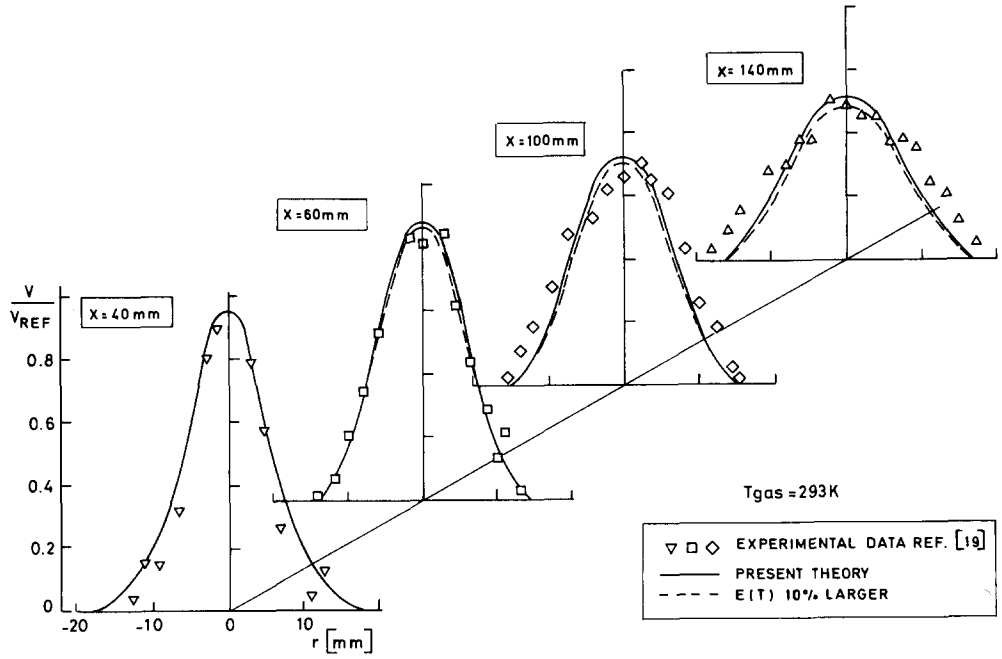

Fig. 3. Downstream changes in volume distribution of droplets produced by an air-kerosene jet atomizer, in a "cold" environment.

due to the latent heat of vaporization. When this factor is taken into consideration, the vaporization rate for the computed steps farther downstream decreases, since vaporization takes place in the cooler environment. (For the "cold" flow, this effect was found to be insignificant.)

Next, the sensitivity of the results to changes in the magnitude of the vaporization-rate coefficient $E(T)$ is examined. Due to the relatively short droplet-residence time, changes of 5–10% in the magnitude of $E(T)$ for kerosene do not cause significant deviations in the downstream

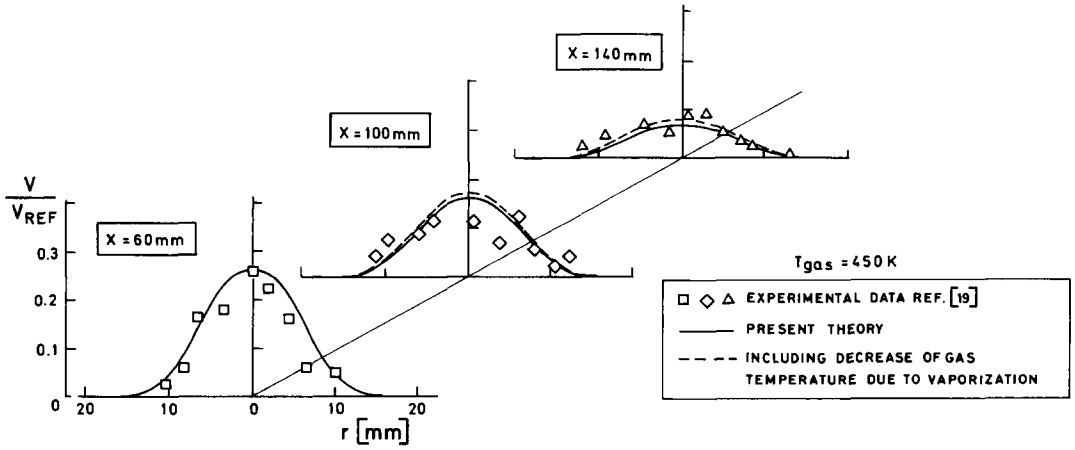

Fig. 4. Downstream changes in volume distribution of droplets produced by an air-kerosene jet atomizer, in a "hot" environment.

droplet volume concentration, even at station x = 140 mm, (see Fig. 3). Thus, computations were also carried out considering two additional vaporization rate coefficients (assuming that the flow conditions remain invariant). These additional coefficients correspond to the following fuel types: dimethyl butane and butanol-1. When compared with kerosene, the vaporization-rate coefficient for the first fuel is considered to be higher by 16% and for the second, butanol-1 fuel, lower by 26.5% [13, 33, 34]. As one may expect, higher vaporization rates result in decreasing droplet volume concentration as one marches downstream, and vice versa for the lower vaporization rates (see Fig. 5).

As to the sensitivity of the results to the magnitude of the effective viscosity and the axial momentum of the jet K', these parameters mainly affect the velocity profile. Larger axial momenta result in higher jet-peak-velocity values (see Fig. 2), while the "width" of the velocity profile increases as the effective viscosity increases (see Fig. 6). However, once the velocity field is computed, the right choice of these values can be verified by comparison with experimental velocity data, as was done in the present study (see Fig. 2).

The effects of effective viscosity on the downstream changes in droplet volume concentration are shown in Fig. 7. As can be seen, only a large increase in the effective viscosity, i.e., by a factor of 1.5–2.5, results in some changes in the droplet volume concentration, especially at the edges of the jet. This is attributed to the fact that the streamlines (carrying the droplets) are shifting from the center of the jet for higher viscosity values and in addition the residence time of the droplets somewhat decreases. Thus, the droplet volume concentration was found to be *insensitive* to small changes in the effective viscosity.

In conclusion, a new Lagrangian sectional method for simulating droplet size distributions of vaporizing fuel sprays suspended in a flow field has been presented. The applicability of this method was demonstrated in a simulation of

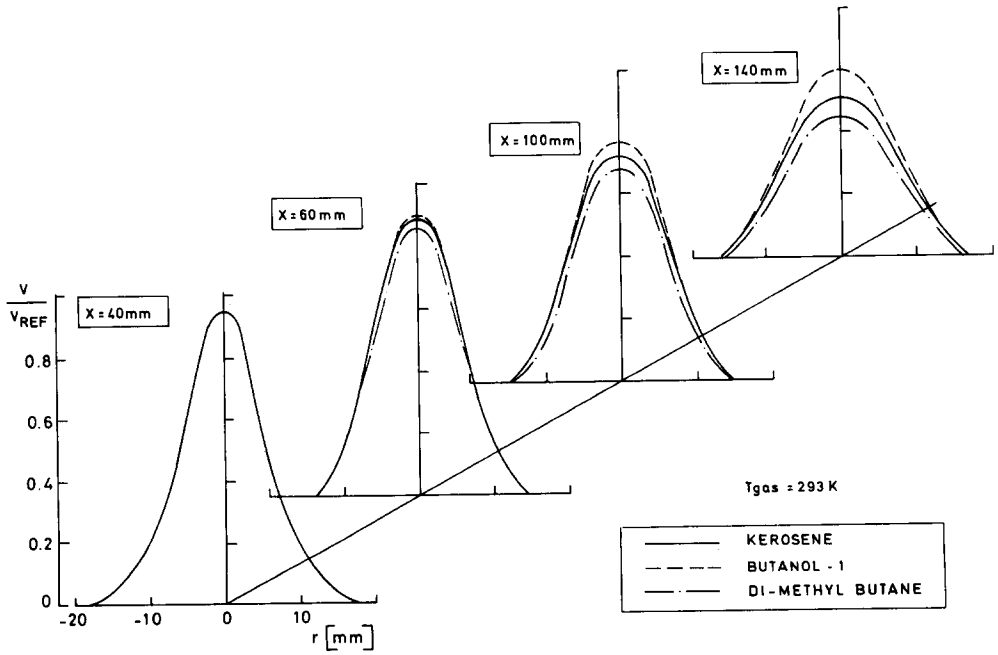

Fig. 5. Downstream changes in volume distribution of droplets in a spray jet for various fuel types, based on the following vaporization-rate coefficients: kerosene, 9.8; butanol-1, 7.2; dimethyl butane, 11.4 ($\times 10^3$ $\mu m^2/s$).

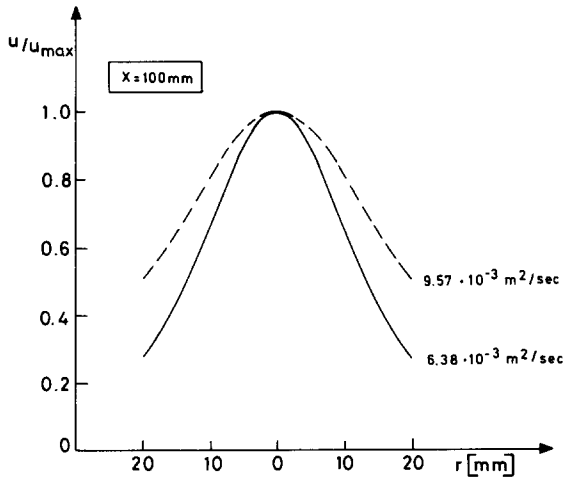

Fig. 6. Effective viscosity effects on the axial velocity profile.

downstream changes in volume distribution of fuel droplets of a spray produced by an air-kerosene jet atomizer.

APPENDIX

A method for estimating the characteristic vaporization rate coefficient $E(T)$ from experimental data showing downstream changes of jet spray characteristics (e.g., Ref. [19]) is presented here.

At the jet's centerline, the variation of the axial velocity with x may be expressed [32] as

$$u_{\text{center}} = \frac{3}{8\pi}\left(\frac{K'}{\nu_{\text{eff}}}\right)\frac{1}{x}. \tag{A.1}$$

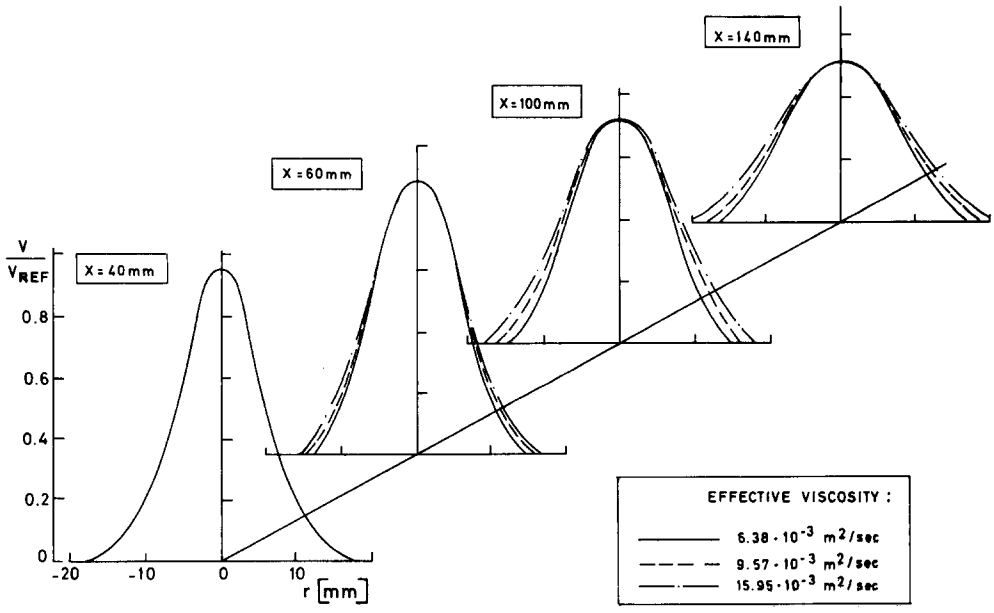

Fig. 7. Effective viscosity effects on the downstream changes in volume distribution of droplets in a kerosene spray jet.

Next, via the distance equation

$$\Delta x = \int_{t_1}^{t_2} u_{\text{center}}\, dt, \tag{A.2}$$

one obtains that the time t varies as

$$t = \frac{1}{2(3/8\pi)(K'/\nu_{\text{eff}})} x^2. \tag{A.3}$$

Now, employing experimental data showing changes in the volume concentration of droplets along the centerline [19], $E(T)$ may be determined as follows. For example, for the "cold" jet, the peak volume concentration varies approximately as x^{-1}, as indicated by Yule et al. [19]. Here we will deal only with *two* peak values at two "stations," e.g., x_1 = 100 mm and x_2 = 140 mm. As will be shown, this information is sufficient to determine $E(T)$.

Next, denoting by N the number concentration of droplets and by $\bar{d}$ the volume mean droplet diameter, the volume vaporization rate may be expressed as [see Eq. (26)]

$$V = -E(T)\frac{\pi}{4}\bar{d}N, \tag{A.4}$$

i.e.,

$$\dot{V}_{x=x_2} = V_{x=x_1} - \int_{t_1}^{t_2} E(T)\frac{\pi}{4} N\bar{d}\, dt. \tag{A.5}$$

Hence, for constant $E(T)$ and constant N (i.e., counting also droplets of zero volume), one obtains

$$E(T) = \frac{4V_{x=x_1}}{\pi N}\left[1 - \frac{V_{x=x_2}}{V_{x=x_1}}\right]\left[\int_{t_1}^{t_2} \bar{d}\, dt\right]^{-1}, \tag{A.6}$$

where the evaluation of the integral in Eq. (A.6) is carried out as follows. Fist, dt is expressed in terms of x via Eq. (A.3). Second, if the mean droplet volume varies as x^{-1}, then the mean volume droplet diameter $\bar{d}$ varies as $x^{-1/3}$. Thus,

$$\int_{t_1}^{t_2} \bar{d}\, dt = \frac{8\pi}{3}\left(\frac{\nu_{\text{eff}}}{K'}\right)\bar{d}_{x=x_1}(x_1)^{1/3}\int_{x_1}^{x_2} x^{2/3}\, dx$$
$$= \frac{8\pi}{5}\left(\frac{\nu_{\text{eff}}}{K'}\right)\bar{d}_{x=x_1}\left[\left(\frac{x_1}{x_2}\right)^{1/3} x_2^2 - x_1^2\right]. \tag{A.7}$$

Next, substituting Eq. (A.7) into (A.6) yields

$$E(T) = \frac{5}{2\pi^2}\left(\frac{K'}{\nu_{\text{eff}}}\right) \times \frac{(V_{x=x_1}/N)}{\bar{d}_{x=x_1}\left[\left(\frac{x_1}{x_2}\right)^{1/3} x_2^2 - x_1^2\right]} \times \left[1 - \frac{V_{x=x_2}}{V_{x=x_1}}\right], \tag{A.8}$$

and since

$$V_{x=x_1} = \frac{\pi}{6}\bar{d}_{x=x_1}{}^3 N, \tag{A.9}$$

Eq. (A.8) finally becomes

$$E(T) = \frac{5}{12\pi}\left(\frac{K'}{\nu_{\text{eff}}}\right) \times \frac{\bar{d}_{x=x_1}{}^2}{[(x_1/x_2)^{1/3} x_2^2 - x_1^2]}\left[1 - \frac{V_{x=x_2}}{V_{x=x_1}}\right]. \tag{A.10}$$

For example, for K' = 6.1414 × 10^{-2} m^4/s^2, ν_{eff} = 6.38 × 10^{-3} m^2/s, x_1 = 0.10 m, x_2 = 0.14 m, $\bar{d}_{x=x_1}$ = 14 μm, and $(V_{x=x_2}/V_{x=x_1})$ = 0.718 (see Figs. 2 and 4 of Ref. [19]), one obtains $E(T)$ = 9.8 × 10^3 $\mu m^2/s$.

REFERENCES

1. Styles, A. C., and Chigier, N. A., *Sixteenth Symposium (International) on Combustion,* The Combustion Institute, Pittsburgh, 1977, pp. 619-630.
2. Chigier, N. A., and McGreath, C. G., *Acta Astronautica* 1:687-710 (1974).
3. Labowski, M., and Rosner, D. E., *Symposium on Evaporation-Combustion of Fuel Droplets,* Division of Petroleum Chemistry, Am. Ch. Soc., 1976.
4. Chiu, H. H., Kim, H. Y., and Croke, E. J., *Nineteenth Symposium (International) on Combustion,* The Combustion Institute, Pittsburgh, 1982, pp. 971-980.
5. Probert, R. P., *Phil Mag.* 37:94 (1946).
6. Tanasawa and Tesim, *Bull. JSME* 1:36 (1958).
7. Nuruzzaman, A. S. M., Siddall, R. G., and Beer, J. M., *Chem. Eng. Sci.* 26:1635 (1971).
8. Mizutani, Y., and Ogasawara, M., *Int. J. Heat and Mass Transfer* 8:921 (1965).

9. Correa, S. M., and Sichel, M., *Nineteenth Symposium (International) on Combustion,* The Combustion Institute, Pittsburgh, 1982, pp. 981-991.
10. Choudhury, P. R., and Gerstein, M., *Nineteenth Symposium (International on Combustion,* The Combustion Institute, Pittsburgh, 1982, pp. 993-997.
11. Tambour, Y., *Isr. J. Tech.* 18:47-56 (1980).
12. Beér, J. M., and Chigier, N. A., *Combustion Aerodynamics,* Applied Science Publishers, London, 1974, pp. 147-195.
13. Williams, A., *Combust. Flame* 21:1-31 (1973).
14. Spalding, D. B., *Combustion and Mass Transfer,* Pergamon Press, 1979, pp. 59-144.
15. Spalding, D. B., *Fourth Symposium on Combustion,* Williams and Wilkins, Baltimore, 1953, pp. 847.
16. Udelson, D., *Combust. Flame* 6:93 (1962).
17. Williams, A., *Combust. Flame* 21:1 (1973).
18. Swithenbank, J., Beér, J. M., Taylor, D. S., Abbot, D., and McCreath, C. G., in *Progress in Astronautics and Aeronautics,* vol. 53 (B. T. Zinn, Ed.), 1977, pp. 421-447.
19. Yule, A. J., Ah Seng, C., Felton, P. G., Ungut, A., and Chigier, N. A., *Combust. Flame* 44:71-84 (1982).
20. Yule, A. J., Ah Seng, C., Felton, P. G., Ungut, A., and Chigier, N. A., *Eighteenth Symposium (International) on Combustion,* The Combustion Institute, Pittsburgh, 1981, pp. 1501-1509.
21. Chigier, N. A., Ungut, A., and Yule, A. J., *Seventeenth Symposium (International) on Combustion,* The Combustion Institute, Pittsburgh, 1979, pp. 315-324.
22. Chigier, N. A., *Combust. Flame* 51:127-139 (1983).
23. Yule, A. J., Ereaut, P. R., and Ungut, A., *Combust. Flame,* 54:15-22 (1983).
24. Tambour, Y., *Combust. Flame* (in press).
25. Patanker, S. V., and Spalding, D. B., *Heat and Mass Transfer in Boundary Layers,* 2nd Ed., Intertext Books, London, 1970.
26. Greenberg, J. B., Tambour, Y., and Gal-Or, B., *Int. J. Heat and Mass Transfer* 23:1595-1598 (1980).
27. Tambour, Y., *The Physics of Fluids* 22:1255-1260 (1979).
28. Polymeropoulos, C. E., *Combust. Sci. and Tech.* 8:111-112 (1973).
29. Law, C. K., and Sirignano, W. A., *Combust. Flame* 28:175-186 (1977).
30. Law, C. K., *Combust. Sci. and Tech.* 15:65-74 (1977).
31. Labowsky, M., *Combust. Sci. and Tech.* 22:217-226 (1980).
32. Schlichting, H., *Boundary Layer Theory,* 7th Ed., McGraw-Hill, New York, 1979, p. 748.
33. Smith, A. L., and Graves, C. C., *NACA,* RME 57, F11, 1957.
34. Wood, B. J., and Wise, H. J., *J. Appl. Phys.* 28:1068 (1957).

Received 29 March 1984; revised 9 October 1984